Supplement of Atmos. Chem. Phys., 22, 13423–13430, 2022
https://doi.org/10.5194/acp-22-13423-2022-supplement

Atmospheric Chemistry and Physics
Open Access

Supplement of

Technical note: Northern midlatitude baseline ozone – long-term changes and the COVID-19 impact

David D. Parrish et al.

Correspondence to: David D. Parrish (david.d.parrish.llc@gmail.com)

Introduction

Three discussion sections are included, which further support and extend the analysis in the manuscript.

S1. Comparison of linear trends derived from power series fit and published linear trend analyses

Estimates of the net, long-term baseline ozone change for progressively longer time periods within the past 3 decades are derived in this work and by Chang et al. (2022). Figure S1 plots nine linear line segments representing independent estimates derived by different approaches and spanning different time intervals. Table S1 gives the parameters defining those line segments, which span the time periods selected for the linear fits. Section S2 investigates how the results of linear regressions depend upon the year selected for beginning the regression.

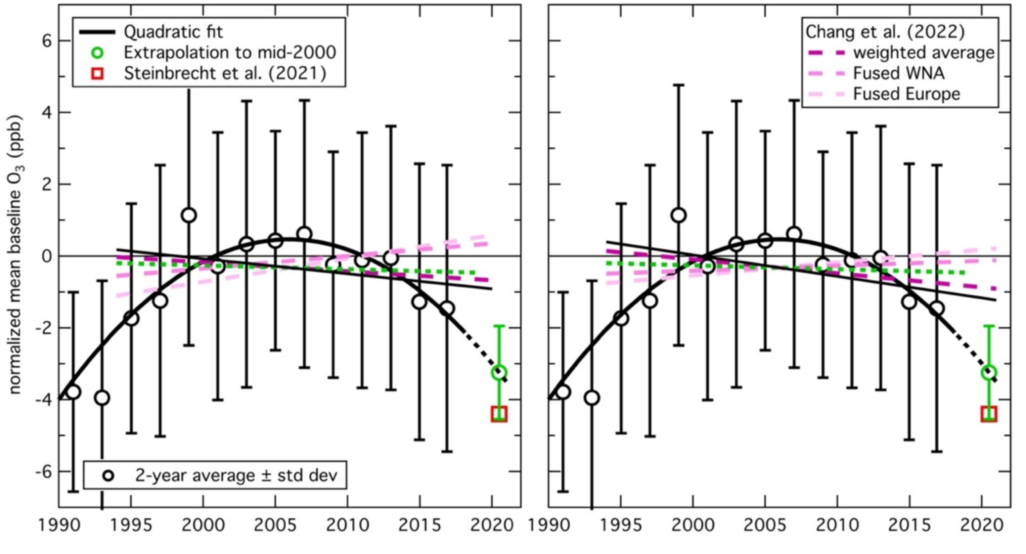

Figure S1. Section of Figure 1 (with axes expanded) comparing linear trends (black line segments) derived from the quadratic fit (black curve), the linear fit to the 1994-2018 monthly means (dotted green line segments) and those derived from Chang et al. (2022) (dashed line segments). The left and right graphs give the Chang et al. (2022) and Equation 2 fits for the 1994-2019 and 1994-2020 periods, respectively. The parameters of all line segments are given in Table S1.

Table S1. Linear trends for baseline ozone at northern mid-latitudes, with estimated 95% confidence limits, and corresponding year 2000 intercepts. To reduce the number of required decimal places the slopes are given in units of ppb/decade, while those in the manuscript are given in units of ppb/year. Corresponding line segments are included in Fig. S1.

Reference	Time Interval	Intercept (ppb)	Trend Slope (ppb/decade)
This work	1994-2018	-0.02 ± 0.02	-0.18 ± 0.89
"	1994-2019	-0.07 ± 0.60	-0.42 ± 0.75
"	1994-2020	+0.04 ± 0.63	-0.60 ± 0.79
Chang et al., 2022 (weighted mean)	1994-2019	-0.17 ± 0.59	-0.25 ± 0.14
"	1994-2020	-0.09 ± 0.60	-0.39 ± 0.30
Chang et al., 2022 (Fused - WNA)	1994-2019	-0.53 ± 0.62	+0.35 ± 0.21
"	1994-2020	-0.41 ± 0.60	+0.14 ± 0.21
Chang et al., 2022 (Fused - Europe)	1994-2019	-0.72 ± 0.68	+0.65 ± 0.19
"	1994-2020	-0.54 ± 0.62	+0.36 ± 0.20

Notes. The 1994-2018 results are from a linear fit to all normalized, deseasonalized monthly means in that time period, with the larger confidence limits from the linear fit to the 2-yean means in the same period; the results from the other two periods are calculated from the quadratic fit (i.e., Equation 2 of the manuscript).

The weighted means for all northern mid-latitude stations of Chang et al. (2022) are discussed in the manuscript; other trends are taken with 2-sigma confidence limits from their Table 2. The intercepts of all the Chang et al. (2022) results are derived by normalizing the line segments to the 1994-2017 2-year means.

S2. Dependence of linear regression results on choice of initial year of the regression

The Conventional Wisdom and the Linear Trend View, unsurprisingly, predict different expectations of the baseline level of ozone in the year 2020. What is required is the time-dependence (trend) of the ozone content during the period preceding the COVID-19 pandemic. The Linear Trend View calculates the average of this trend (i.e., slope) over significant time scales and assumes this constant value to be the local value pre-COVID. The Conventional Wisdom, on the other hand, fits the evident long-term, non-linear behavior to give an extrapolated value for the trend appropriate for the pre-COVID period. The major weakness in the Linear Trend View is clear when non-linear behavior exists - the value of the calculated trend depends on the time period chosen for the linear fit; since the data in Figure 1 have sequential ascending and descending legs, this average will necessarily underestimate the local pre-COVID trend. The major weakness in the Conventional Wisdom model is that the data contain substantial variability (inherent in atmospheric phenomena) and the quadratic term necessary to calculate the quantitative pre-COVID rate of decrease has substantial statistical uncertainty. To illustrate this issue a cursory piece-wise linear trend analysis of the 2-year means plotted in Figure 1 is given here.

Linear approximations are typically applied to a non-linear function to obtain local derivatives of that function, in the spirit of the origins of the Calculus, that is by taking the limit of $\Delta f(x)/\Delta x$ as Δx approaches zero. Here we apply this approach to illustrate the slope of the non-linear ozone change expected in the year 2000 had the COVID-19 pandemic not occurred. A linear regression of the average ozone data values in Figure 1 produces the graph in Figure S2 when the regression interval is varied. Each symbol with error bar shows the slope from a regressed linear trend derived over a shrinking time period (from a given start year to the most recent 2-year mean (2017)) is analyzed. The standard error bars of these regressed slopes arise from the scatter in the averages themselves, not from the standard deviations of the monthly means included in the individual 2-year averages, which are indicated by the error bars in Figure 1.

Three results are apparent from this analysis:

(1) The non-linearity of the data is obvious. The regressed linear slope from the 2-year means depends on the time interval of the data regressed and clearly shows the historic change from an increasing average ozone trend (positive slope) over the entire time period to a decreasing average trend (negative slope) over the period beginning in the mid-1990s, when the time period before the ozone maximum decreases to match the time after the maximum. The green triangles indicate the of starting dates for the trends given in the Linear Trend View references; they are mostly near the time of this crossover, thus resulting in small derived positive or negative trends. Further, these green triangles, although exhibiting significant scatter, also show a tendency to decrease with a later starting year; the green dotted line indicates the linear regression to those triangles, which gives a slope (-0.020 ± 0.023 ppb yr^{-2}), which is nearly significant at the 95% confidence lever and agrees well with the slope from the quadratic fit, -0.018 ± 0.06 ppb yr^{-2}, i.e. the *c* parameter from Equation 1 of the manuscript.

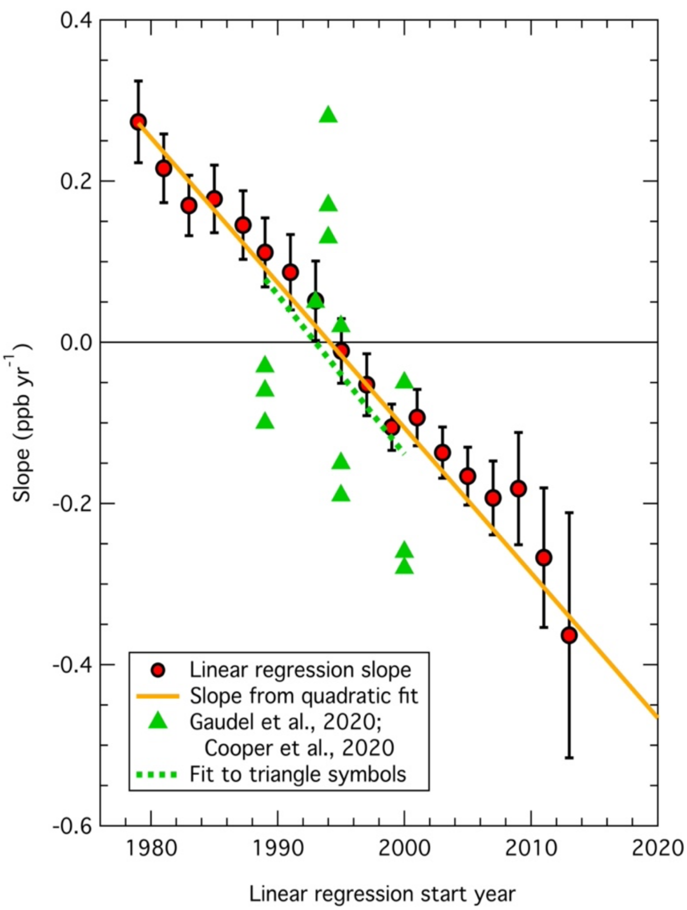

(2) The quadratic fit given by Equation 1 discussed in the manuscript necessarily implies that the slope over any selected time interval specified by t_1 and t_2 is equal to $b + c*(t_1 + t_2)$. The gold line in Figure S2 is derived from the parameter values discussed in the manuscript and $t_2 = 17$, i.e. the t value for the most recent (2017) 2-year average. There is only small variability of the individual regressed slopes about this line, which is a strong indication of the fidelity with which the quadratic fit describes the overall non-linear long-term ozone changes. Notably, the few slopes derived after a linear regression start time of the mid-

Figure S2. Dependence of slope of linear regressions derived from the 2-year means included in Figure 1 compared to trends derived from two of the Linear Trend View papers. Symbols with error bars give slopes with standard errors derived from linear regressions to all 2-year means (left point) and to progressively one fewer 2-year means (points moving progressively to the right). Line indicates the slope dependence expected from quadratic fit plotted in Figure 1. Triangles give northern midlatitude free troposphere trends reported by Gaudel et al. (2020) in their Table S1a and northern midlatitude surface site trends reported by Cooper et al. (2020) in their Table 2. The dotted green line is the linear regression to the triangles.

2000s are based only on measurements after the quadratic fit reached is maximum, which indicates that the quadratic fit not only accurately describes the early ozone increases, but also accurately describes recent ozone decreases as well.

(3) The approximately linear nature of the derived derivatives is a further demonstration that higher order terms in the power series fitting procedure are not statistically significant.

Cursory use of this Newtonian (Leibniz) variation of the Linear Trend treatment yields a conservative linear trend (derivative) of -0.4 ppb/yr for the most recent segments of the data. With an ozone deficit of -1.6 ppb apparent in 2017, linear extrapolation of this value for 3 years at -0.4 ppb per year yields an estimated ozone burden in 2020 which is 2.8 ppb lower than the pre-COVID average used by Steinbrecht et al. (2021). This value is close to the 3.2 ppb value obtained from the integral treatment described in the manuscript and explains 70% of the 4 ppb difference discussed by Steinbrecht et al., 2021.

S3. Preliminary analysis of Western US CASTNET data covering the Covid-19 period

The analysis illustrated in Figure 1 of the manuscript is based on measurement records that extend only through 2017; analysis of data sets that include more recent measurements would provide more accurate and precise estimates of the COVID impact. However, some of the data sets utilized by Parrish et al. (2020) have not yet been archived and made publicly available for years after 2017, so it is not yet possible to add additional data to those shown in Figure 1. However, one relevant ozone data set is available that has been updated through 2021 – the Clean Air Status and Trends Network (CASTNET) of the US EPA (https://www.epa.gov/castnet; last accessed 27 August 2022), which includes sites in the Western US that have been interpreted as baseline representative. Here we investigate ozone measurements from seven of the western US CASTNET sites (locations shown in inset map in Figure S3), which are chosen to be as isolated as possible from anthropogenic emission sources, and to span a wide latitude range (32° to 48.5° N). All are at similar elevations (2.0 ± 0.43 km) except Glacier NP at 0.96 km.

Data from most of these same CASTNET sites have been included in a series of studies of long-term ozone changes at western US rural and remote sites. Jaffe et al. (2003), Jaffe and Ray (2007), Parrish et al. (2009; 2012; 2014; 2017; 2020) and Cooper et al. (2014) have investigated Lassen Volcanic NP data, due to the site's location near the US West Coast. Jaffe and Ray (2007) also considered three of the other sites (Glacier NP, Yellowstone NP and Canyonlands NP). Two other sites (Great Basin NP and Grand Canyon NP) were considered by Cooper et al. (2020) in their analysis of surface ozone trends at globally distributed remote sites. Here we include an additional, more southerly site (Chiricahua NM) in Arizona. To our knowledge, these data sets include all of the longest, high quality ozone data sets collected at relatively isolated rural sites in the western continental US.

The time series of the annual means of the maximum daily 8-hr average (MDA8) ozone at the seven CASTNET sites are illustrated in the upper graph of Figure S3; curves showing regression fits for each site to Equation 1 are included. The derived parameter values are included in Table S2, along with confidence limits and the root-mean-square deviation (RMSD) of the annual mean MDA8s from the fits. The MDA8s recorded in the year 2020 are excluded from all fits, since those data may have been significantly affected by the COVID-19 related emissions reductions. The derived *a* coefficient values are similar at all sites except for the northern, lower elevation Glacier NP site. The derived *b* and *c* coefficients agree at all sites within their confidence limits, although many values are not significantly different from zero, and at the Glacier NP site both coefficients appear smaller than at the other sites. This agreement indicates that there is no statistically significant difference in the temporal evolution of the MDA8s recorded at any of these widely separated, western US sites.

The similarity of the temporal evolution of these rural ozone concentrations suggests adopting the analysis of Parrish et al. (2020) by normalizing the annual mean MDA8s to remove the spatial variability and to derive a single fit of Equation 1 to all MDA8s from the seven sites. We proceed by subtracting the derived *a* coefficient values from the respective MDA8 time series in order to normalize each fit to 0 ppb in the year 2000. As shown in the lower panel of Figure S3 and in Table S2, the 189 normalized annual mean MDA8s recorded over 32 years at the seven sites are fit within a RMSD of 1.6 ppb. The non-linear behavior, similar to that shown in Figure 1 is evident to the eye - the collected data scatter around zero in the middle years while remaining below zero for the early and later periods. The fit to the combined data set gives $b = 0.11 \pm 0.06$ ppb yr^{-1} and $c = -0.010 \pm 0.003$ ppb yr^{-2}; all of the *b* and *c* parameters derived from the separate fits at the seven sites agree with these values within their confidence limits. Also included in Figure S3 is a fit to a cubic polynomial (dotted curve), which shows discernable differences from the quadratic fit (solid line), although the cubic coefficient $(+2.7 \pm 4.1) \times 10^{-4}$ ppb yr^{-3} is not significantly different from zero. These parameter values indicate that the rural MDA8s increased early in the data records with a positive slope in the year 2000, reached a maximum in $year_{max} = 2005 \pm 3$, and decreased thereafter -behavior that closely parallels that of the baseline ozone data illustrated in Figure 1 of the manuscript.

The *b* and *c* parameter values derived here from the normalized CASTNET annual mean MDA8s are similar, but not quite in agreement within derived confidence limits (see Table S2) with the parameter values derived for the entire northern midlatitudes (Parrish et al., 2020) from baseline ozone data; the present parameter values are only ~50 to 55% of the Parrish et al. (2020) values. The cause of this difference is uncertain at present; however we do note that Glacier NP appears to exhibit significantly different behaviour; if that site is excluded, then the $b = 0.13 \pm 0.06$ ppb yr^{-1} and $c = -0.012 \pm 0.004$ ppb yr^{-2} parameters of the quadratic fit are somewhat larger; furthermore a cubic fit gives a statistically significant cubic parameter coefficient $(+5.6 \pm 4.0) \times 10^{-4}$ ppb yr^{-3} and a larger $c = -0.023 \pm 0.009$ ppb yr^{-2}, which agrees with the $c = -0.018 \pm 0.008$ ppb yr^{-2} derived from the baseline data. Further investigation is required before we can consider the analysis of these CASTNET data to be clearly understood. Nevertheless, this preliminary analysis shows a strong quantitative agreement to the functional form of the trend in Figure 1 and furthermore, indicates its continuation through the Covid -19 period.

The quadratic fits in Figure S3 exclude the data from the year 2020; thus, the deviations of the year 2020 MDA8s from those fits provide quantitative estimates of the COVID-19 impact at these baseline-representative sites. The year 2020 deviations from the overall fit at the seven CASTNET sites range from -2.5 to +1.9 ppb with a mean of -0.5 ± 1.2 ppb. This estimate of the COVID-19 impact on baseline ozone concentrations at northern midlatitudes agrees (within the derived uncertainty limits) with the COVID-19 impact estimate derived from the extrapolation of the baseline ozone data (-1.2 ± 1.3 ppb) given in the manuscript. This agreement of the CASTNET data analysis (which extends through 2021) with the results of the extrapolation of the baseline data, which do not extend past 2017, strongly supports the extrapolation analysis presented in the manuscript.

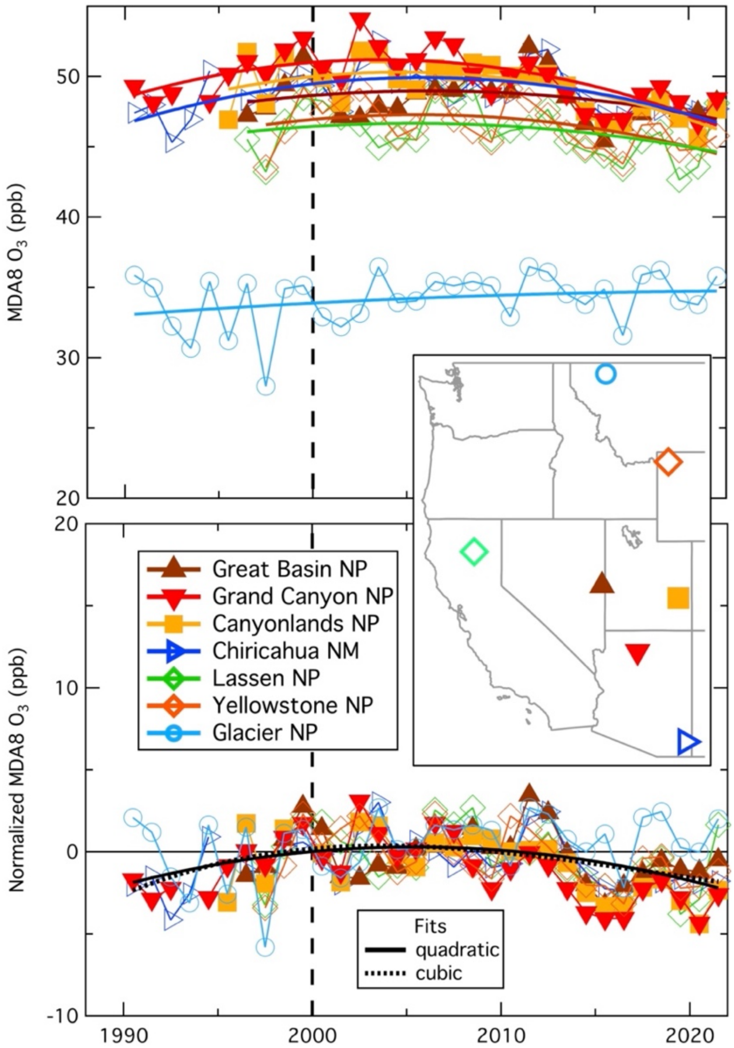

Figure S3. Time series of annual mean MDA8 ozone recorded at the seven rural western CASTNET sites shown in the inset map. Solid curves indicate the fits of Equation 1 to the individual site time series (upper panel) and to all normalized data (black curve, lower panel). Dotted curve in lower panel shows the fit to a cubic polynomial.

One cautionary note should be added to the CASTNET data analysis; it assumes that 2021 was a "COVID-free" year as far as ozone production is concerned and as such provides a "bracket" around 2020. The world economy had recovered during 2021 raing global GDP 2.4% higher than it was in 2019, more than making up for the 3.3% drop in 2020 (World Bank, 2022), supporting this assumption. The COVID-19 pandemic continued through 2021 however, and activity in some sectors, civil aviation in particular, (IATA, 2022) remained depressed. Therefore, there may be a residual bias in the 2021 data. To check for such a possiblity, we performed the same analysis as illustrated in Figure S3 except for omitting both 2020 and 2021 in the quadratic fit, thus using only the trend established up to 2019 - the eve of the Covid-19 pandemic. By extrapolating this trend by one year, we obtain a prediction for 2020 to compare with the 2020 observations. This approach gives results (mean of +0.1 ± 1.2 ppb) that agree with the above within the specified confidence limits. Thus, the CASTNET trends obtained both with and without the 2021 data are consistent with each other, and with the results from the non-linear trend extrapolation used in the manuscript.

Table S2. Parameter values (with 95% confidence limits) derived from fits of Equation 1 to time series of annual mean MDA8 time series from the isolated rural CASTNET sites compared to the baseline ozone results of Parrish et al. (2020). The year 2020 MDA8s are excluded from the CASTNET fits.

Site	*a* (ppb)	*b* (ppb yr^{-1})	*c* (ppb yr^{-2})	$year_{max}$	RMSD (ppb)
Glacier NP	33.8 ± 1.0	0.06 ± 0.13	-0.001 ± 0.010	1954 ± 694	1.9
Yellowstone NP	46.9 ± 1.2	0.12 ± 0.29	-0.011 ± 0.015	2006 ± 15	1.6
Lassen Volcanic NP	46.5 ± 1.2	0.09 ± 0.28	-0.008 ± 0.015	2005 ± 19	1.8
Great Basin NP	48.7 ± 1.1	0.11 ± 0.25	-0.009 ± 0.013	2006 ± 17	1.6
Canyonlands NP	50.0 ± 0.8	0.14 ± 0.19	-0.015 ± 0.010	2005 ± 7	1.3
Grand Canyon NP	51.0 ± 0.7	0.10 ± 0.10	-0.015 ± 0.007	2004 ± 4	1.4
Chiricahua NM	49.5 ± 0.7	0.15 ± 0.09	-0.013 ± 0.007	2006 ± 5	1.3
All sites - normalized	0.0 ± 0.3	0.11 ± 0.06	-0.010 ± 0.003	2005 ± 3	1.6
Baseline ozone results	0.0 ± 0.1	0.20 ± 0.06	-0.018 ± 0.006	2006 ± 3	1.4

References

Cooper, O. R., et al. (2014). Global distribution and trends of tropospheric ozone: An observation-based review. *Elem Sci Anth* 2: 29. DOI: https://doi.org/10.12952/journal.elementa.000029

Cooper, O. R., et al. (2020). Multi-decadal surface ozone trends at globally distributed remote locations, *Elem. Sci. Anth., 8*, 23. doi.org/10.1525/elementa.420

Iata data: https://www.iata.org/en/iata-repository/pressroom/fact-sheets/industry-statistics, 2022

Jaffe, D., Price, H., Parrish, D. D., Goldstein, A., & Harris, J. (2003). Increasing background ozone during spring on the west coast of North America, *Geophysical Research Letters, 30*(12), 1613. doi.org/10.1029/2003GL017024

Jaffe, D. A., and J. Ray (2007), Increase in Ozone at Rural Sites in the Western U.S., *Atmos. Environ., 41*, 5452–5463.

Parrish, D. D., Millet, D. B., & Goldstein, A. H. (2009). Increasing ozone in marine boundary layer air inflow at the west coasts of North America and Europe, *Atmospheric Chemistry and Physics,* 9, 1303–1323

Parrish, D. D., Law, K. S., Staehelin, J., Derwent, R., Cooper, O. R., Tanimoto, H., et al. (2012). Long-term changes in lower tropospheric baseline ozone concentrations at northern mid-latitudes. Atmospheric Chemistry and Physics, 12, 11,485–11,504. https://doi.org/10.5194/acp-12-11485-2012

Parrish, D. D., Lamarque, J. F., Naik, V., Horowitz, L., Shindell, D. T., Staehelin, J., et al. (2014). Long-term changes in lower tropospheric baseline ozone concentrations: Comparing chemistry-climate models and observations at northern midlatitudes. Journal of Geophysical Research: Atmospheres, 119, 5719–5736. https://doi.org/10.1002/2013JD021435

Parrish, D. D., Petropavlovskikh, I., & Oltmans, S. J. (2017). Reversal of long-term trend in baseline ozone concentrations at the North American west coast. Geophysical Research Letters, 44, 10,675–10,681. https://doi.org/10.1002/2017GL074960

Parrish, D. D., et al. (2020), Zonal similarity of long-term changes and seasonal cycles of baseline ozone at northern midlatitudes. J. Geophys. Res.: Atmos., doi: 10.1029/2019JD031908.

World Bank Open Data: https://data.worldbank.org/indicator/NY.GDP.MKTP.KD.ZG (in constant 2015 US$), 2022